



Research Article

# Synthesis, Characterization and Applications of (*E*)-3-((5-bromo-2-hydroxy-3-methoxycyclohexa-1,3-dienyl)methyleneamino)-6-(hydroxymethyl)-tetrahydro-2*H*-pyran-2,4,5-triol

Solomon Tadesse<sup>1</sup>, Yelda Bingöl Alpaslan<sup>2</sup>, Mustafa Yıldız<sup>3,4</sup>✉, Hüseyin Ünver<sup>5</sup>, Kadir Aslan<sup>1</sup>✉<sup>1</sup>Morgan State University, Department of Chemistry, 1700 East Cold Spring Lane, Baltimore, MD 21251, USA.<sup>2</sup>Department of Biophysics, Faculty of Medicine, Giresun University, Giresun, Turkey.<sup>3</sup>Department of Chemistry, Faculty of Arts and Sciences, Çanakkale Onsekiz Mart University, 17100 Çanakkale, Turkey.<sup>4</sup>Nanoscience and Technology Research and Application Center (NANORAC), Çanakkale Onsekiz Mart University, Çanakkale, Turkey.<sup>5</sup>Department of Physics, Faculty of Science, Ankara University, 06100 Besevler-Ankara, Turkey.

✉ Corresponding authors. E-mail: myildiz@comu.edu.tr; kadir.aslan@morgan.edu

**Received:** Mar. 15, 2016; **Accepted:** May 10, 2016; **Published:** May 13, 2016.**Citation:** Solomon Tadesse, Yelda Bingöl Alpaslan, Mustafa Yıldız, Hüseyin Ünver and Kadir Aslan, Synthesis, Characterization and Applications of (*E*)-3-((5-bromo-2-hydroxy-3-methoxycyclohexa-1,3-dienyl)methyleneamino)-6-(hydroxymethyl)-tetrahydro-2*H*-pyran-2,4,5-triol. *Nano Biomed. Eng.*, 2016, 8(2): 72-81.**DOI:** 10.5101/nbe.v8i2.p72-81.

## Abstract

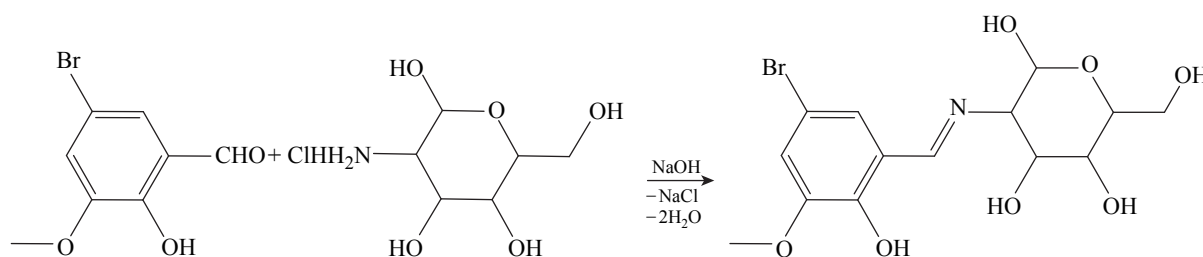
We present the synthesis, characterization, biological and sensing applications of a Schiff base, (*E*)-3-((5-bromo-2-hydroxy-3-methoxycyclohexa-1,3-dienyl)methyleneamino)-6-(hydroxymethyl)-tetrahydro-2*H*-pyran-2,4,5-triol. Characterization of the title compound was carried out using theoretical quantum-mechanical calculations and experimental spectroscopic methods. The molecular structure of the title compound was confirmed using NMR and FTIR, which was in good agreement with the structure predicted by the theoretical calculations. The title compound was evaluated for its ability to detect anions in DMSO and on a solid surface and for its antimicrobial activity against several common microorganisms.

**Keywords:** Schiff base;  $\alpha$ -D-Glucosamine; Density functional theory; Anion sensing; Antimicrobial activity

## Introduction

Schiff bases continue to attract the attention of numerous research groups around the world due to their ability to bind DNA and anions and act as antimicrobial agents [1]-[7]. The synthesis of Schiff bases involve the condensation of carbonyl groups and primary amines. In Schiff bases derived from

aldehydes containing an ortho-hydroxy group, two types of tautomeric forms are observed: phenol-imine and keto-amine. The presence of these tautomeric forms can be confirmed using <sup>13</sup>C-NMR, <sup>1</sup>H-NMR, UV-vis spectroscopy and X-ray crystallography [8]-[15]. Tautomerism occurs due to the transfer of O-H proton to imine nitrogen (-C=N) in 2-Hydroxy Schiff bases and results in the modifications of their



**Scheme 1** The synthesis of the title compound.

electronic structures. In this regard, Schiff bases can be employed as anion sensors due to these intramolecular hydrogen bond and proton transfer process [16]-[19]. More specifically, keto-amine and enol-imine tautomer equilibrium is the main reason for the selective bond formation between Schiff bases and anions.

Earlier attempts to synthesize Schiff bases from the reactions of glucosamine and salicylaldehyde employed sodium bicarbonate as the reaction medium. Several research groups also reported the synthesis of azomethines and imines of the glucosamine [1], [3]-[7], [20]-[23]. However, the preparation of Schiff bases from the reactions of glucosamine with benzaldehyde and veratraldehyde and glucosamine with vanillin and 5-bromosalicylaldehyde are still challenging [5]. In order to alleviate this problem, in this work, we employed 3-methoxy-5-bromosalicylaldehyde derivative of glucosamine as a starting material for successful formation of Schiff derivative of D-glucosamine with an aldehyde containing the abovementioned substituents. D-glucosamine was chosen for its bioavailability and biocompatibility. D-glucosamines can bind DNA and can be taken up by microorganisms.

A Schiff base, (*E*)-3-((5-bromo-2-hydroxy-3-methoxycyclohexa-1,3-dienyl) methyleneamino)-6-(hydroxymethyl)-tetrahydro-2*H*-pyran-2,4,5-triol (Scheme 1), was synthesized from the reaction of 3-methoxy-5-bromosalicylaldehyde with  $\alpha$ -D-glucosamine hydrochloride and was characterized using spectroscopic methods. The antimicrobial activity of the title compound was investigated to determine its minimum inhibitory concentration (MIC) against several microorganisms. Theoretical calculations were carried out to predict the molecular geometry, vibrational frequencies, UV-Visible, HOMO-LUMO energies, natural bond orbital analysis (NBO) and nonlinear optics (NLO) properties of the compound using DFT/B3LYP method with 6-311++G(d,p) basis set in ground state. The experimental and calculated spectroscopic data of the compound were found to be

in a good agreement. The colorimetric response of the Schiff base receptors in DMSO was investigated. The compound displayed a color change upon addition of  $\text{CN}^-$ ,  $\text{AcO}^-$ ,  $\text{F}^-$ ,  $\text{OH}^-$ , and  $\text{H}_2\text{PO}_4^-$  with a substantial bathochromic shift from 340 to 425 nm. No color change was observed upon addition of  $\text{Br}^-$ ,  $\text{I}^-$ ,  $\text{ClO}_4^-$ ,  $\text{N}_3^-$ ,  $\text{CNS}^-$  and  $\text{HSO}_4^-$ . The most discernable color change in the title compound was caused by  $\text{CN}^-$ , which demonstrated that the title compound can be used to selectively detect  $\text{CN}^-$  in DMSO and on a solid surface. The order of anion-binding power of the title compound was determined to be  $\text{CN}^- \sim \text{AcO}^- > \text{F}^- > \text{OH}^- > \text{H}_2\text{PO}_4^-$ . In addition, in order to investigate the interaction between receptor and anion, the  $^1\text{H-NMR}$  titration was employed.

## Materials and Methods

### Materials

D-glucosamine hydrochloride, 5-bromo-3-methoxysalicylaldehyde, NaOH, MeOH, DMSO,  $\text{CHCl}_3$ , n-pentane and tetrabutylammonium salts (fluoride, bromide, iodide, cyanide, thiocyanate, perchlorate, hydrogen sulphate, acetate, azide, dihydrogen phosphate, hydroxide) were purchased from Aldrich. Solid surfaces (chromatography paper, 3 mm thick, Catalog Number: 3030-6187) were purchased from Whatman International Ltd., England.

The  $^1\text{H}$  and  $^{13}\text{C}$  NMR spectra were recorded in  $\text{DMSO-}d_6$  on a Bruker AVANCE-400 spectrometer operating at 400 and 1016 MHz. Infrared absorption spectra were obtained from a Agilent Cary 630 FTIR spectrometer and were reported in  $\text{cm}^{-1}$  units. The UV-VIS spectra were measured using AGILENT Cary 60 series spectrometer. Melting points were measured on a MEL-TEMP II apparatus using a capillary tube.

### Synthesis of (*E*)-3-((5-bromo-2-hydroxy-3-methoxycyclohexa-1,3-dienyl) methyleneamino)-6-(hydroxymethyl)-tetrahydro-2*H*-pyran-2,4,5-triol

D-glucosamine hydrochloride (1.00 g; 4.63 mmol), NaOH (0.1855 g; 4.63 mmol) and 3-methoxy-5-bromosalicylaldehyde (1.069 g; 2.73 mmol) were added to a 250 mL round-bottomed flask. The mixture was stirred and refluxed for 2 h. The solid was filtered and washed with water and methanol. The product was obtained pure enough. It was crystallized from  $\text{CHCl}_3$  : n-pentane (3:1) as a yellow solid, m.p. 115 °C, 1.39 g (76%) yield. Found: C, 42.85; H, 4.62; N, 3.57. Calc. For  $\text{C}_{14}\text{H}_{18}\text{BrNO}_7$ ; C, 42.87; H, 4.59; N, 3.57%.  $^1\text{H-NMR}$  (DMSO);  $\delta$  ppm, 10.46 (s, 1H, Ar-OH); 10.23-9.34 (s, 3H, Alif-OH); 9.33 (s, 1H, Ar-CH=N-); 7.38-6.56 (m, 2H, Ar-H); 3.88-3.46 (m, 8H, Alif-H); 3.36 (s, 3H, -OCH<sub>3</sub>) (Fig. S1).  $^{13}\text{C-NMR}$  (DMSO);  $\delta$  ppm, 68.6 (s, 1C, C1); 71.10 (s, 1C, C2); 73.1 (s, 1C, C3); 77.3 (s, 1C, C4); 92.6 (s, 1C, C5); 66.1 (s, 1C, C6); 189.7 (s, 1C, C7); 131.9 (s, 1C, C8); 153.8 (s, 1C, C9); 160.1 (s, 1C, C10); 121.1 (s, 1C, C11); 118.1 (s, 1C, C12); 123.7 (s, 1C, C13); 56.2 (s, 1C, C14) (Fig. S2).

### NMR titration

Three NMR tubes of Schiff base dissolved in DMSO- $d_6$  were prepared and then different equivalents (0.0, 0.5 and 3.0 equiv.) of tetraethylammonium fluoride dissolved in DMSO- $d_6$  were added to two solution of Schiff base tube. After shaking thoroughly,  $^1\text{H}$  NMR spectra were taken at room temperature.  $^1\text{H}$  NMR titrations were carried out in DMSO- $d_6$  (Fig. S1). As seen in Fig. S1(a), the free compound showed three peaks at 10.46, 10.23 and 9.34 ppm, which could be ascribed to -OH protons. The fluoride ions is mixed (0.5 equiv), the -OH peak intensity decreases (S1(b)). When fluoride ion was introduced (3.0 equiv), the signals at 10.46, 10.23 and 9.34 ppm disappeared, indicating the -OH moiety of the compound acted as anion binding sites and exhibited deprotonation upon interacting with strong basic anions. Therefore, the significant red shifts in absorption and color changes resulted from deprotonation of the anion binding sites [24, 25].

### FT-IR studies

FT-IR spectrum of the investigated compound was measured in the 4000-600  $\text{cm}^{-1}$  region using ATR on Agilent Cary 630 FTIR spectrometer (Fig. S3) and the vibrational frequencies of the compound were calculated by using B3LYP/6-311++G(d,p) method. Additionally, theoretical vibrational frequencies of the

compound were interpreted by means of PEDs using VEDA 4 program [Vibrational energy distribution analysis VEDA 4, Warsaw]. The observed vibration bands were assigned and compared with the calculated frequencies. The experimental and calculated vibrational frequencies and their assignments are given in Table S1. The visual checks for the vibrational band assignments were also performed by using Gauss-View molecular visualization program.

### Computational procedures

The optimized molecular structure, vibrational wavenumber, UV-vis spectroscopic parameters, frontier molecular orbital analyses, natural bond orbital analysis (NBO) and nonlinear optics (NLO) properties of the compound have been calculated by using DFT/B3LYP method with 6-311++G(d,p) basis set. In the DFT calculations, B3LYP (Becke's three parameter hybrid functional using the LYP correlation functional) was performed employing the Berny method [26] at 6-311++G(d,p) basis set [27]. This process was performed with the Gaussian 09 software package [Gaussian, Inc., Wallingford CT] and GaussView 5 visualization program [GaussView, Version 5.0.9, Semichem Inc., Shawnee Mission, KS, 2009].

### Screening for antimicrobial activities

MIC was evaluated by broth micro dilution test. A loop full of bacteria was inoculated in 100 mL of nutrient broth at 37 °C for 20 h in a test-tube shaker at 150  $\text{rev min}^{-1}$ . The test compounds were prepared by dissolving in a minimal volume of DMSO and were serially diluted in Mueller-Hinton broth at concentrations in the range of 1-500  $\mu\text{g/mL}$ . The 24-h bacterial cultures were then transferred into 10 mL of the Muller-Hinton broth (control and test compounds) and incubated at 37 °C for 24 h. The growth of bacteria was determined by measuring the turbidity after 24 h. Thus, the MIC was generally read as the smallest concentration of the drug in the series that prevents the development of visible growth of the test organism.

*Bacillus subtilis* ATCC 6633, *Saphylococcus aureus* ATCC 25923, *Enterococcus faecalis* ATCC 29212, *Escherichia coli* ATCC 25922, *Pseudomonas aeruginosa* ATCC 254992, *Bacillus cereus* NRRL B-3704, *Proteus vulgaris* ATCC 13315, *Candida albicans* ATCC 60193, and *Candida tropicalis* ATCC 13803 were used as microorganisms. Gentamicin, ampicillin and fluconazol were used as controls in

this study as they are well-known broad-spectrum antibiotics that have different mechanisms of activity, such as interruption of protein synthesis (gentamicin) and inhibition of cell wall synthesis (ampicillin) [28]. The compounds were dissolved in DMSO (dimethyl sulfoxide) to a final concentration of 500  $\mu\text{g/mL}$ . The concentration of the compounds on different plates was 500  $\mu\text{g/mL}$ , 250  $\mu\text{g/mL}$ , 125  $\mu\text{g/mL}$ , 62.5  $\mu\text{g/mL}$ , 31.25  $\mu\text{g/mL}$ , 15.6  $\mu\text{g/mL}$ , 8  $\mu\text{g/mL}$ , 4  $\mu\text{g/mL}$ , 2  $\mu\text{g/mL}$ , and 1  $\mu\text{g/mL}$ .

## Results and Discussion

### Optimized geometry

The optimized molecular structure at the B3LYP/6-311G++(d,p) level of the title compound is shown in Fig. 1(a). The calculated molecular geometric parameters at the B3LYP/6-311G++(d,p) level are listed in Table S1. The C–C bond lengths in phenyl rings of the title molecule were calculated at the interval 1.375–1.418 Å and the calculated C5–O11, C4–O13 and O13–C14 bond lengths were found as 1.339 Å, 1.355 Å and 1.421 Å, respectively. The O11–C5–C6, C4–O13–C14 and N10–C9–C6 bond angles were calculated as 122.65°, 118.51° and 122.69° for the compound, respectively. The O11–N10 bond length was found as 2.625 Å. This bond length is shorter than Van der Waals radius of the N and O atoms [3.07 Å] [29]. In addition, the N10–C9 bond lengths were calculated 1.281 Å and the O11–H12...N10 bond

angles were calculated as 147.46°. These results show that intramolecular hydrogen bonding can be formed in this region between O11 and N10 atoms. As a result of geometric optimization,  $\alpha$ -D-glucosamine part of the compound were optimized at chair conformation. Additionally, the C–O bond lengths in  $\alpha$ -D-glucosamine part of the molecule were calculated at the interval 1.410–1.436 Å and C24–O36–C22 bond angles was computed as 117.60°. The longest bond length in the molecule was found in C2–Br1 and it was calculated as 1.919 Å.

### UV-visible and HOMO–LUMO analyses

The UV-vis electronic absorption spectrum of the compound in DMSO was recorded within 200–800 nm at the room temperature. The UV-visible spectrum of o-hydroxylated Schiff bases that exist mainly as the phenol-imine structure indicate the presence of a band at <400 nm, whereas compounds existing in the keto-amine form show a new band, especially in polar and non-polar solvents at >400 nm [30]. Electronic absorption spectra of the title compound in DMSO solvent show a band at 350 nm, which corresponds to the enol-imine form. This value for related compounds is similar to in the literature [31]. However, the compound showed no absorption above 400 nm. This indicates that the title compound is in the enol-imine form in DMSO solvent. Electronic absorption spectra of the compound were calculated by using TD-DFT method based on the B3LYP/6-311++G(d,p) level optimized structure in gas phase.

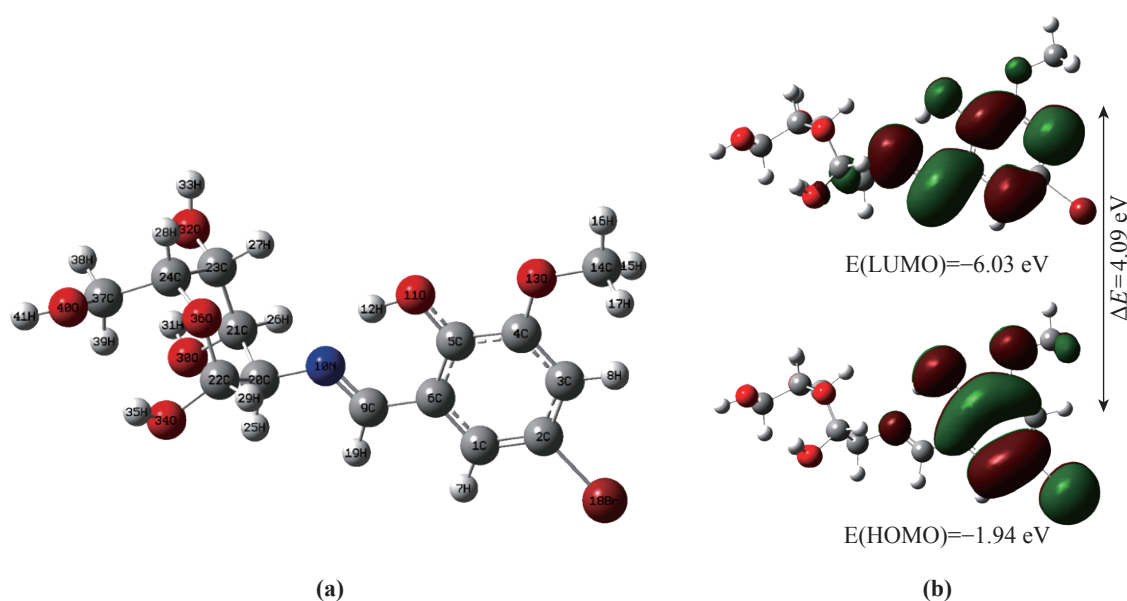


**Fig. 1** (a) The theoretical geometric structure of the title compound (at B3LYP/6-311++G(d,p) level). (b) Molecular orbital surfaces and energy levels for the HOMO, LUMO of the title compound computed at B3LYP/6-311++G(d,p).

The TD-DFT theoretical absorption band calculations obtained at 347.74/339.05 (in vacuum/DMSO). The bands are corresponded to transitions. The highest occupied molecular orbital (HOMO) represents the outermost orbital filled by electrons and behaves as an electron donor, while the lowest unoccupied molecular orbital (LUMO) considers as the first empty innermost orbital unfilled by electron and behaves as an electron acceptor. These orbitals are also called as frontier molecule orbitals (FMOs). The energy gap between HOMO and LUMO indicates the molecular chemical stability and is a critical parameter to determine molecular electrical transport properties [32]. In our study, HOMO and LUMO energies and their 3D plots of the compound are shown in Fig 1(b). As seen from Fig. 1(b), HOMO and LUMO electrons are localized over the phenyl ring and azomethine group. Depending on HOMO and LUMO values,  $I$  (ionization potential),  $A$  (electron affinity),  $\chi$  (electronegativity),  $\eta$  chemical hardness,  $\zeta$  (softness) and  $\psi$  (electrophilicity index) parameters are given in Table S2 [33].

### FT-IR studies

The OH stretching mode can be observed in the range of  $2800\text{ cm}^{-1}$  to  $3500\text{ cm}^{-1}$ , depending on intra- and inter-molecular hydrogen bonding and is very sensitive due to the environmental factors. Free OH stretching vibrations give rise to sharp bands in the region  $3500\text{--}3700\text{ cm}^{-1}$ , while the OH stretching modes under intra- and inter-molecular hydrogen bonding interaction observe as mixed with other vibrational bands at the interval  $2800\text{--}3200\text{ cm}^{-1}$  [34]. The OH stretching bands of  $\alpha$ -D-glucosamine group of the title compound are not observed in IR spectrum. However, these bands are computed in the region  $3626.02\text{--}3688.72\text{ cm}^{-1}$ . Similarly, the O11–H12 stretching vibrational band under intra-molecular hydrogen bonding interaction is not observed in IR spectrum, while this band is calculated at  $3055.13$  and  $3058.68\text{ cm}^{-1}$  with 87% and 12% contributions of PED, respectively. The experimental and calculated wavenumbers of other bands belonged to OH vibrational of the title compound are given in Table S1.

The aromatic (with  $sp^2$  hybrid) and aliphatic (with  $sp^3$  hybrid) CH stretching modes observe in the regions  $3000\text{--}3100\text{ cm}^{-1}$  and  $2800\text{--}3000\text{ cm}^{-1}$  [35]. The CH stretching bands in phenyl ring of the title compound are not observed in IR spectrum, while these bands are found at  $3058.68$  and  $3087.67\text{ cm}^{-1}$  with PED

contributions of 86% and 98%, respectively. The observed bands at  $2941$  and  $2836\text{ cm}^{-1}$  can be assigned to CH stretching bands in aliphatic groups of title compound. The scissoring modes of methyl group are found at  $1479.86\text{ cm}^{-1}/57\%$ ,  $1473.81\text{ cm}^{-1}/22\%$  and  $1460\text{ cm}^{-1}/1467.63\text{ cm}^{-1}/95\%$ , while the symmetric bending vibrations of this group are computed at  $1469.86\text{ cm}^{-1}/23\%$  and  $1449.68\text{ cm}^{-1}/57\%$  (exp./cal./PED). Similarly, the rocking modes for methyl group are calculated at  $1186.46$  and  $1147.79\text{ cm}^{-1}$  with 66% and 74% contributions of PED, respectively. The N=C stretching vibration, which is most characteristic band of the Schiff base derivatives, occur in the region  $1500\text{--}1700\text{ cm}^{-1}$  [34]. The azomethine N=C stretching vibration is observed at  $1655\text{ cm}^{-1}$ , while the calculated value of this band is found at  $1655.18\text{ cm}^{-1}$  with 69% contribution of PED. Similarly, the C–C stretching bands in aromatic ring are found at  $1605\text{ cm}^{-1}/1623.20/25\%$  and  $1573\text{ cm}^{-1}/1575.71\text{ cm}^{-1}/42\%$  (exp./cal./PED). The stretching bands of O11–C5 bond are found at  $1259/1284.55\text{ cm}^{-1}/42\%$  (exp./cal./PED). Similarly, the O–C stretching vibrations for O–C bonds of  $\alpha$ -D-glucosamine group are experimentally observed at  $1082$  and  $1023\text{ cm}^{-1}$  and they are theoretically computed in the region below  $1092.29\text{ cm}^{-1}$ . The observed band at  $959\text{ cm}^{-1}$  is assigned to symmetric stretching mode of  $-\text{C}-\text{O}-\text{CH}_3$  group with PED contribution of 26%, while asymmetric one this group is calculated at  $1119.02\text{ cm}^{-1}$  with PED contribution of 22% [36].

### NBO analysis

The NBO analysis is an efficient method for understanding of intra- and inter-molecular bonding, bond species, and interactions among bonds, hyperconjugation interactions or charge transfers (ICT) in molecular systems. Additionally, the NBO gives remarkable information about the interactions between Lewis type (bonding or lone pair) filled orbitals and non-Lewis type (antibonding or Rydberg) vacancy orbitals. The  $E(2)$ , the hyperconjugative interaction energy or the stabilization energy, shows intensity of interaction between donor groups and acceptor ones. Delocalization of electron density between occupied Lewis type orbitals and formally unoccupied non-Lewis orbitals correspond to a stabilizing donor-acceptor interaction. For each donor NBO ( $i$ ) and acceptor NBO ( $j$ ), the stabilization energy  $E(2)$  associated with electron delocalization between donor and acceptor is estimated as [37],

$$E(2) = -q_i \frac{F_{ij}^2}{\Delta E} = -q_i \frac{\langle i|F|j \rangle^2}{\varepsilon_j - \varepsilon_i} \quad (1)$$

where  $q_i$  is the donor orbital occupancy,  $\varepsilon_i$  and  $\varepsilon_j$  are diagonal elements (orbital energies), and  $F_{ij}$  is the off-diagonal NBO Fock matrix element. The results of second-order perturbation theory analysis of the Fock Matrix at the B3LYP/6-311++G(d,p) level of theory are given in Table S3. The stabilization energy values greater than 4 kcal mol<sup>-1</sup> are listed in Table S3. The strongest hyperconjugation interactions are appeared in n(O11)→ $\pi^*$ (C5-C6) [ $E(2) = 37.06$  kcal mol<sup>-1</sup>, ED(i) = 1.80757e, ED(j) = 0.42805e] and n(O13)→ $\pi^*$ (C3-C5) [ $E(2) = 30.98$  kcal mol<sup>-1</sup>, ED(i) = 1.83468e, ED(j) = 0.36526e] transitions. The n→ $\sigma^*$  transitions in the title molecule are found in n(O36)→ $\sigma^*$ (C22-O34) [ED(i) = 1.90014e and ED(j) = 0.05205e] and n(N10)→ $\sigma^*$ (C9-H19) [ED(i) = 1.86700 e and ED(j) = 0.03920e] with stabilization energy values of 13.58 and 11.01 kcal mol<sup>-1</sup>. Additionally, the intra molecular hydrogen bonding n(N10)→ $\sigma^*$ (O11-H12) transition as an evidence of enol form of molecule is found at 23.82 kcal mol<sup>-1</sup>, ED(i) = 1.86700e and ED(j) = 0.06477e values. The  $\pi$ → $\pi^*$  transitions are in C1-C2→C3-C4/C5-C6, C3-C4→C1-C2/C5-C6 and C5-C6→C1-C2/C3-C4/C9-N10 transitions with stabilization energy values of 17.36/1453, 11831/17.94 and 21.98/16.94/20.05 kcal mol<sup>-1</sup>, respectively. Similarly, the strongest hyperconjugation interaction in  $\sigma$ → $\sigma^*$  transition is found in C37-O4 [ED = 1.99426e]→O40-H41 [ED = 0.00462e] with the  $E(2)$  energy value of 10.74 kcal mol<sup>-1</sup>.

### Colorimetric anion sensing in solution and on solid surfaces

The chromogenic sensing ability of the title compound was evaluated first using tetrabutylammonium salts of a series of anions including F<sup>-</sup>, Br<sup>-</sup>, I<sup>-</sup>, CN<sup>-</sup>, SCN<sup>-</sup>, ClO<sub>4</sub><sup>-</sup>, HSO<sub>4</sub><sup>-</sup>, AcO<sup>-</sup>, N<sub>3</sub><sup>-</sup>, H<sub>2</sub>PO<sub>4</sub><sup>-</sup>, OH<sup>-</sup> in DMSO solutions and UV-vis spectroscopy (Figures 2(a) and 2(b)). Upon the addition of 1 equivalent of each anion, only F<sup>-</sup>, CN<sup>-</sup>, AcO<sup>-</sup>, H<sub>2</sub>PO<sub>4</sub><sup>-</sup>, OH<sup>-</sup> resulted in the disappearance of the main absorption band at 425 nm, which can be attributed to the hydrogen bonds between the title compound and the anions and to the resultant charge transfer processes in the title compound. On the other hand, the addition of other anions did not induce any spectral changes in the title compound (Fig. 2(b)).

In order to investigate whether the title compound can be used for visual confirmation of anions in a

solution, the real color photographs of the solutions of the title compound with the above-mentioned anions are taken and shown in Figure 2(a). After the anions are added to the title compound in DMSO, the color of the solution was changed from dark yellow to light yellow only with AcO<sup>-</sup> and CN<sup>-</sup> dark yellow and light yellow with F<sup>-</sup>, OH<sup>-</sup>, H<sub>2</sub>PO<sub>4</sub><sup>-</sup>, with fast response time (<1 sec), indicating that receptor the title compound can serve as a “naked-eye” indicator for CN<sup>-</sup>, AcO<sup>-</sup>, F<sup>-</sup>, OH<sup>-</sup> and H<sub>2</sub>PO<sub>4</sub><sup>-</sup> in DMSO. The high selectivity of the title compound for CN<sup>-</sup> and AcO<sup>-</sup> may be due to the nucleophilicity of these anions in DMSO. The order of selectivity or the binding affinity of anions for the title compound is CN<sup>-</sup>~AcO<sup>-</sup> > F<sup>-</sup> > OH<sup>-</sup> > H<sub>2</sub>PO<sub>4</sub><sup>-</sup> >> Br<sup>-</sup>~I<sup>-</sup>~SCN<sup>-</sup>~ClO<sub>4</sub><sup>-</sup>~HSO<sub>4</sub><sup>-</sup>~N<sub>3</sub><sup>-</sup>.

The potential use of the title compound as a solid-state sensor by colorimetric measurements was demonstrated. In this regard, the title compound was sensitive to CN<sup>-</sup> and OH<sup>-</sup> on a solid surface. Figure 3 shows that the color of the solid state sensor changed yellow immediately after the addition of CN<sup>-</sup> in water (100 M, pH = 7), and showed no color change when other anions were added. We also observed that OH<sup>-</sup> can potentially interfere in the measurements for CN<sup>-</sup> in water. These investigations are ongoing and will be resulted in due course.

It is important to comment on the mechanism of anion binding to the title compound. The more acidic hydroxyl proton is deprotonated upon exposure to more basic OH<sup>-</sup>, F<sup>-</sup>, AcO<sup>-</sup> and H<sub>2</sub>PO<sub>4</sub><sup>-</sup> ions and therefore, the intramolecular proton transfer occurs to the keto-amine form [24] (Scheme 2(a)). The formation of keto-amine form of the title compound leads to higher wavelength absorption. The presence of other anions tested with dissimilar basicity with OH<sup>-</sup>, F<sup>-</sup>, AcO<sup>-</sup> and H<sub>2</sub>PO<sub>4</sub><sup>-</sup> such as, Br<sup>-</sup>, I<sup>-</sup>, S<sup>-</sup>, CN<sup>-</sup>, ClO<sub>4</sub><sup>-</sup>, HSO<sub>4</sub><sup>-</sup> and N<sub>3</sub><sup>-</sup> did not result in similar absorption. In contrast, cyanide has much weaker hydrogen bonding ability in comparison with F<sup>-</sup>, OH<sup>-</sup> and H<sub>2</sub>PO<sub>4</sub><sup>-</sup> and stronger nucleophilicity toward the imine group, which results in the addition reaction of CN<sup>-</sup> to the carbon atom of an electron deficient imine group and subsequently, fast proton transfer of the phenol hydrogen to the neighboring nitrogen anion through an intramolecular hydrogen bond (Scheme 2(b)). The addition of up to 12 equivalent of CN<sup>-</sup>, AcO<sup>-</sup>, F<sup>-</sup>, OH<sup>-</sup> and H<sub>2</sub>PO<sub>4</sub><sup>-</sup> ions to a solution of the title compound resulted in a decrease of absorption band at 351 nm and the appearance of a new band at 425 nm, indicative of the conversion of the title compound into the title compound-ion complex, as shown in Figure 2(b).

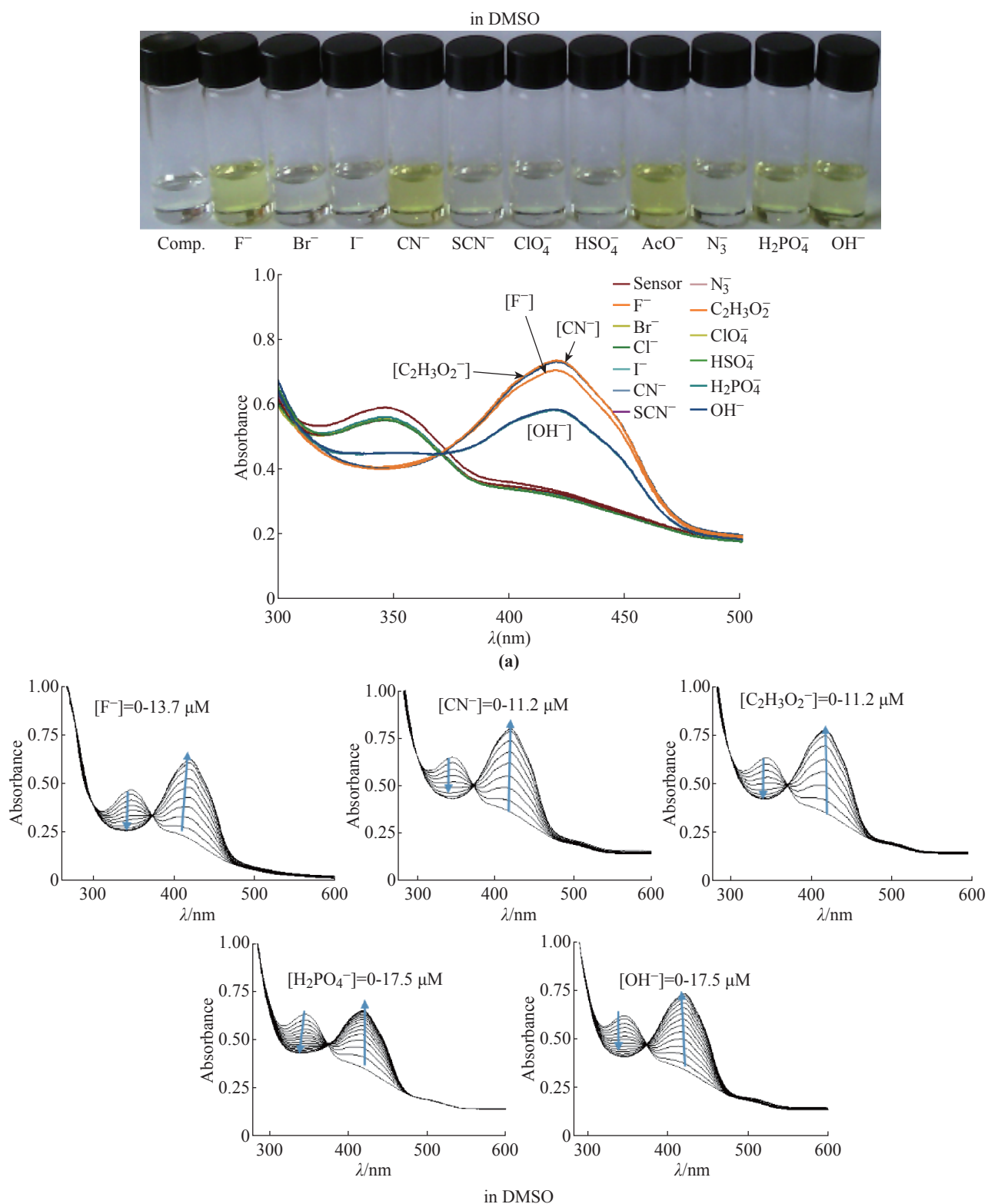


**Fig. 2 (a)** The color changes of the compound (1 equiv) upon addition of various anions (3 equiv) of the compound in DMSO. **(b)** UV-vis spectra of compound (50  $\mu\text{M}$ ) upon the addition of 3 equiv of  $\text{CN}^-$ ,  $\text{AcO}^-$ ,  $\text{F}^-$ ,  $\text{OH}^-$ ,  $\text{H}_2\text{PO}_4^-$ ,  $\text{Br}^-$ ,  $\text{I}^-$ ,  $\text{SCN}^-$ ,  $\text{ClO}_4^-$ ,  $\text{HSO}_4^-$ ,  $\text{N}_3^-$ , **(c)** UV-vis spectra of compound (50  $\mu\text{M}$ ) upon the addition of increasing concentration of  $\text{CN}^-$ ,  $\text{F}^-$ ,  $\text{AcO}^-$ ,  $\text{OH}^-$  and  $\text{H}_2\text{PO}_4^-$ , in DMSO. Arrows show the increased direction of anions.

### Minimum inhibitory concentration (MIC)

MIC was evaluated by broth micro dilution test

and the results are reported in Table S5 (from three separate experiments). The title compound shows high antimicrobial activity against *C. albicans* ATCC

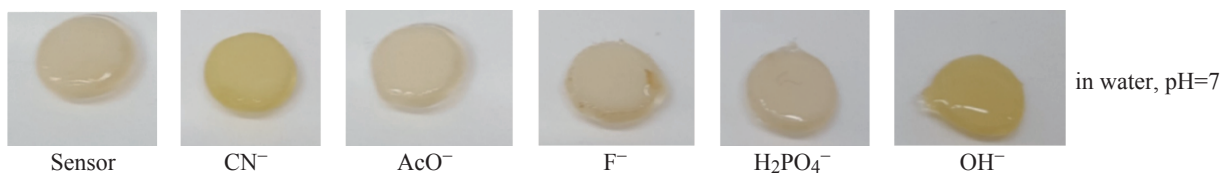
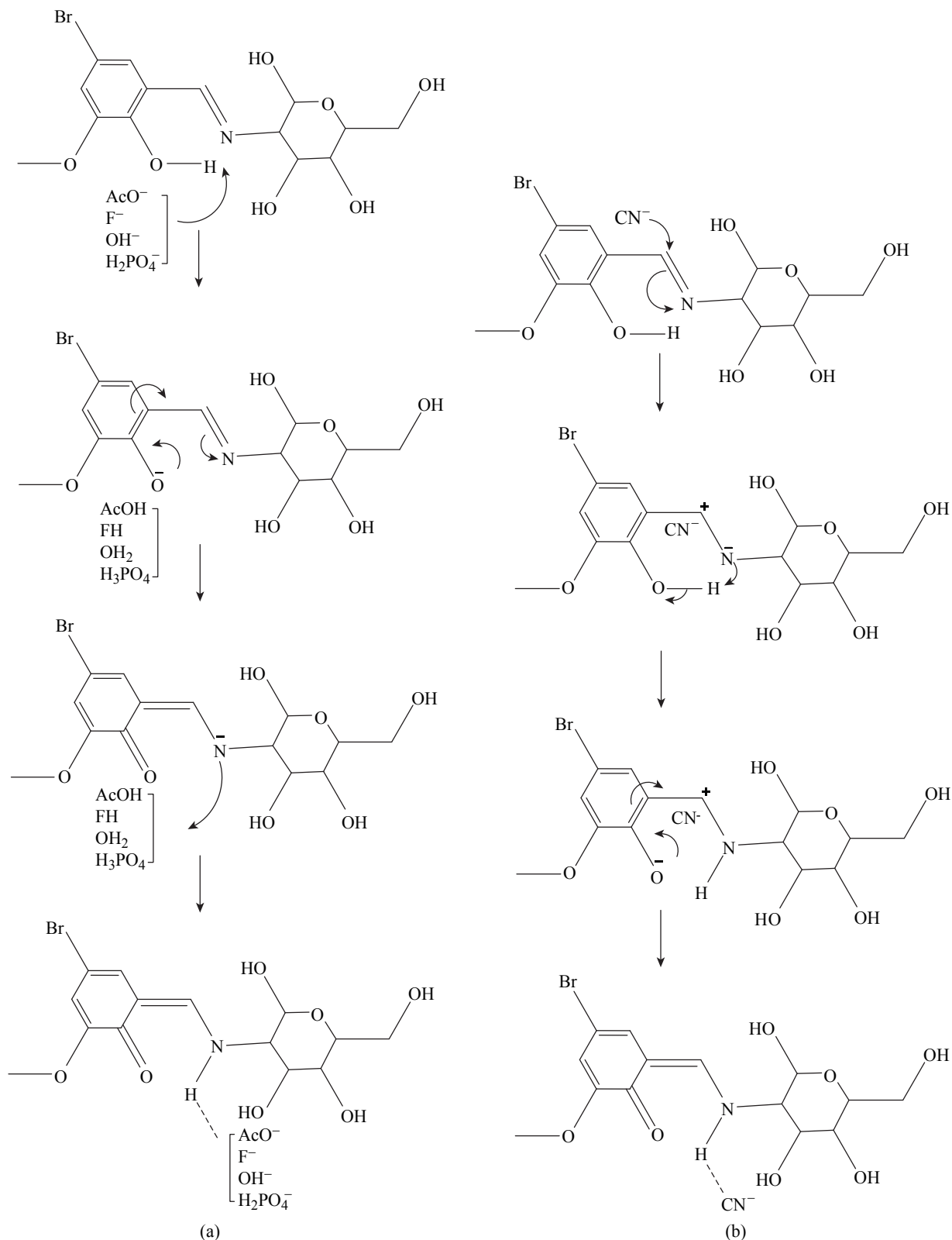


Fig. 3 Solid state application of the title compound.



Scheme 2 The proposed sensing mechanism of the title compound for AcO<sup>-</sup>, F<sup>-</sup>, OH<sup>-</sup>, H<sub>2</sub>PO<sub>4</sub><sup>-</sup> and CN<sup>-</sup> anions in DMSO.

60193 (Table S5). The title compound showed stronger antibacterial effect against and high bacterial effect on *E. faecalis* ATCC 29212 and *B. subtilis* ATCC 6633 compared to *S. aureus* ATCC 25923, *E. coli* ATCC 25922, *E. coli* NRRL B-3704 and *P. vulgaris* ATCC 13315. However, the title compound showed no effect on *P. aeruginosa* ATCC 254992. The title compound differs significantly in its activity against tested microorganisms, which may be attributed to the fact that the cell wall in Gram-positive bacteria are of a single layer, whereas the Gram-negative cell wall is a multilayered structure, and the yeast cell wall is quite complex. Several *C. albicans* species have shown resistance to antifungal drugs [38].

## Conclusions

The synthesis, characterization and applications of (*E*)-3-((5-bromo-2-hydroxy-3-methoxycyclohexa-1,3-dienyl)methyleneamino)-6-(hydroxymethyl)-tetrahydro-2*H*-pyran-2,4,5-triol were reported. Theoretical calculations showed the title compound can potentially be used in applications of non-linear optics. Theoretical and experimental investigations were carried out to validate the intra- and inter-molecular bonding and anion sensing mechanisms. The title compound was able to selectively recognize  $\text{AcO}^-$ ,  $\text{F}^-$ ,  $\text{OH}^-$ ,  $\text{H}_2\text{PO}_4^-$  and  $\text{CN}^-$  anions in DMSO, which was confirmed by colorimetric studies. The potential use of the title compound as a solid state sensor for the detection of  $\text{CN}^-$  anions in water was also demonstrated. The title compound showed strong antimicrobial activity against several common microorganisms.

## Acknowledgments

The authors are grateful to the Scientific Research Project Office of Giresun University, Turkey, for access to the Gaussian 09W program package (Project no: FEN-BAP-A-220413-61) and the Scientific and Technical Research Council of Turkey (TÜBİTAK) for the financial support of this work, grant number BİDEB-2221.

## Supplementary Data

Supplementary data (experimental procedures,  $^{13}\text{C}$ -NMR, FT-IR, absorption spectroscopic data)

associated with this article can be found, in the online version.

## References

- [1] M.R.E. Aly, R.R. Schmidt, New diacylamino protecting groups for glucosamine. *European Journal of Organic Chemistry*, 2005, 2005(20): 4382-4392.
- [2] A.N. Bedekar, A. N. Naik and A.C. Pise, Schiff base derivatives of 2-Amino-2-deoxy-1,3,4,6-tetra-O-acetyl- $\beta$ -D-glucopyranose. *Asian J. Chem*, 2009, 21(9): 6661-6666.
- [3] J. Costamagna, L.E. Lillo, B. Matsuhira, et al., Ni(II) complexes with Schiff bases derived from amino sugars. *Carbohydr Res*, 2003, 338(15): 1535-1542.
- [4] J.C. Irvine, J.C. Earl, Salicylidene derivatives of d-glucosamine. *Journal of the Chemical Society, Transactions*, 1922, 121: 2376.
- [5] B. Kołodziej, E. Grech, W. Schilf, et al., Anomeric and tautomeric equilibria in d-2-glucosamine Schiff bases. *Journal of Molecular Structure*, 2007, 844-845: 32-37.
- [6] D.T. Nguyen, V. Q. Nguyen, Study on synthesis of 2-(Substituted Benzylidene)amino-2-Deoxy-1,3,4,6-Tetra-O-Acetyl- $\beta$ -D-Glucopyranoses from D-Glucosamine. *Letters in Organic Chemistry*, 2013, 10(2): 85-90.
- [7] E.M. Perez, M. Avalos, R. Babiano, et al., Schiff bases from D-glucosamine and aliphatic ketones. *Carbohydr Res*, 2010, 345(1): 23-32.
- [8] M. Gavrančić, B. Kaitner, E. Meštrović, Intramolecular N-H...O hydrogen bonding, quinoid effect, and partial  $\pi$ -electron delocalization in N-aryl Schiff bases of 2-hydroxy-1-naphthaldehyde: the crystal structures of planar N-( $\alpha$ -naphthyl)- and N-( $\beta$ -naphthyl)-2-oxy-1-naphthalimine. *Journal of Chemical Crystallography*, 1996, 26(1): 23-28.
- [9] B. Kaitner, G. Pavlovic, A reinvestigation of the quinoid effect in N-n-Propyl-2-oxo-1-naphthylidenemethylamine. *Acta Crystallographica Section C Crystal Structure Communications*, 1996, 52: 2573-2575.
- [10] H. Nazir, M. Yıldız, H. Yılmaz, et al., Intramolecular hydrogen bonding and tautomerism in Schiff bases. Structure of N-(2-pyridil)-2-oxo-1-naphthylidenemethylamine. *Journal of Molecular Structure*, 2000, 524: 241-250.
- [11] H. Ünver, M. Yıldız, Tautomerism in solution and solid state, spectroscopic studies and crystal structure of (Z)-1-[(4-amino-2,3,5,6-tetramethylphenylamino)methylene]-1,8a-dihydronaphthalen-2(3H)-one. *Spectroscopy Letters*, 2010, 43(2): 114-121.
- [12] H. Ünver, M. Yıldız, D.M. Zengin, et al., Intramolecular hydrogen bonding and tautomerism in N-(3-pyridil)-2-oxo-1-naphthylidenemethylamine. *Journal of Chemical Crystallography*, 2001, 31(4): 211-216.
- [13] M. Yıldız, Synthesis and spectroscopic studies of some new polyether ligands of the Schiff base type. *Spectroscopy Letters*, 2004, 37(4): 367-381.
- [14] M. Yıldız, Z. Kılıç, T. Hökelek, Intramolecular hydrogen bonding and tautomerism in Schiff bases. Part I. Structure of 1,8-di[N-2-oxyphenyl-salicylidene]-3,6-dioxaoctane. *Journal of Molecular Structure*, 1998, 441(1): 1-10.
- [15] M. Yıldız, H. Ünver, D. Erdener, et al., Tautomeric properties and crystal structure of N-[2-hydroxy-1-naphthylidene]2,5-dichloroaniline. *Crystal Research and Technology*, 2006, 41(6): 600-606.
- [16] R. Arabahmadi, S. Amani, A new fluoride ion colorimetric sensor based on azo-azomethine receptors. *Supramolecular Chemistry*, 2014, 26(5-6): 321-328.

- [17] S. Guha, S. Saha, Fluoride ion sensing by an anion- $\pi$  interaction. *J Am Chem Soc*, 2010, 132(50): 17674-17677.
- [18] G. Liu, J. Shao, Ratiometric fluorescence and colorimetric sensing of anion utilizing simple Schiff base derivatives. *Journal of Inclusion Phenomena and Macrocyclic Chemistry*, 2013, 76(1): 99-105.
- [19] D. Sharma, A.R. Mistry, R.K. Bera, et al., Spectroscopic and computational studies on the development of simple colorimetric and fluorescent sensors for bioactive anions. *Supramolecular Chemistry*, 2013, 25(4): 212-220.
- [20] E.A. Dikusar, V.I. Potkin, N.G. Kozlov, Synthesis of water-soluble azomethines based on the substituted benzaldehydes of vanillin series and D-(+)-glucosamine hydrochloride. *Russian Journal of General Chemistry*, 2009, 79(12): 2655-2657.
- [21] D.B.T. Ngo, H.T. Ho, Nguyen, Q.V. Nguyen, et al., Investigation of synthetic reaction of azomethines from glucosamine and substituted benzaldehydes. Proceedings of the 15th Int. Electron. Conf. Synth. Org. Chem. November 2011: 1-30.
- [22] A.K. Sah, C.P. Rao, P.K. Saarenketo, et al., Synthesis, characterisation and crystal structures of Schiff bases from the reaction of 4,6-O-ethylidene- $\beta$ -D-glucopyranosylamine with substituted salicylaldehydes. *Carbohydrate Research*, 2001, 335(1): 33-43.
- [23] F. Safoura, Novel synthesis of Schiff bases bearing glucosamine moiety. *Res. J. Chem. Sci.*, 2014, 4(2): 25-28.
- [24] B. Barare, M. Yıldız, G. Alpaslan, et al., Synthesis, characterization, theoretical calculations, DNA binding and colorimetric anion sensing applications of 1-[(E)-[(6-methoxy-1,3-benzothiazol-2-yl)imino]methyl]naphthalen-2-ol. *Sensors and Actuators B: Chemical*, 2015, 215: 52-61.
- [25] M. Yıldız, Ö. Karpuz, C.T. Zeyrek, et al., Synthesis, biological activity, DNA binding and anion sensors, molecular structure and quantum chemical studies of a novel bidentate Schiff base derived from 3,5-bis(trifluoromethyl)aniline and salicylaldehyde. *Journal of Molecular Structure*, 2015, 1094: 148-160.
- [26] A.D. Becke, Density-functional thermochemistry. III. The role of exact exchange. *The Journal of Chemical Physics*, 1993, 98: 5648.
- [27] C. Peng, P.Y. Ayala, H.B. Schlegel, et al., Using redundant internal coordinates to optimize equilibrium geometries and transition states. *Journal of Computational Chemistry*, 1996, 17(1): 49-56.
- [28] F. Li, M. Feterl, Y. Mulyana, et al., In vitro susceptibility and cellular uptake for a new class of antimicrobial agents: dinuclear ruthenium(II) complexes. *J Antimicrob Chemother*, 2012, 67(11): 2686-2695.
- [29] A. Bondi, Van der Waals volumes and radii. *The Journal of Physical Chemistry*, 1964, 68(3): 441-451.
- [30] S.R. Salman, F.S. Kamounah, Mass spectral study of tautomerism in some 1-hydroxy-2-naphthaldehyde schiff bases. *Spectroscopy Letters*, 2002, 35(3): 327-335.
- [31] A.A. Ađar, H. Tanak, M. Yavuz, Experimental and quantum chemical calculational studies on 2-[(4-propylphenylimino)methyl]-4-nitrophenol. *Molecular Physics*, 2010, 108(13): 1759-1772.
- [32] I. Fleming, Frontier orbitals and organic chemical reactions. John Wiley & Sons. John Wiley & Sons, 1976.
- [33] A. Soltani, F. Ghari, A.D. Khalaji, et al., Crystal structure, spectroscopic and theoretical studies on two Schiff base compounds of 2,6-dichlorobenzylidene-2,4-dichloroaniline and 2,4-dichlorobenzylidene-2,4-dichloroaniline. *Spectrochim Acta A Mol Biomol Spectrosc*, 2015, 139: 271-278.
- [34] R.M. Silverstein, F.X. Webster, D.J. Kiemel, Spectroscopic identification of organic compounds. John Wiley & Sons. John Wiley & Sons, 2005.
- [35] B.H. Stuart, InfraRed spectroscopy: fundamentals and applications. John Wiley & Sons. John Wiley & Sons, 2004.
- [36] H. Gökce, O. Akyildirim, S. Bahçeli, et al., The 1-acetyl-3-methyl-4-[3-methoxy-4-(4-methylbenzoxy)benzylideneamino]-4,5-dihydro-1H-1,2,4-triazol-5-one molecule investigated by a joint spectroscopic and quantum chemical calculations. *Journal of Molecular Structure*, 2014(1), 1056-1057: 273-284.
- [37] C. James, A.A. Raj, R. Reghunathan, et al., Structural conformation and vibrational spectroscopic studies of 2,6-bis(p-N,N-dimethyl benzylidene)cyclohexanone using density functional theory. *Journal of Raman Spectroscopy*, 2006, 37(12): 1381-1392.
- [38] T.C. White, S. Holleman, F. Dy, et al., Resistance mechanisms in clinical isolates of *Candida albicans*. *Antimicrob Agents Chemother*, 2002, 46(6): 1704-1713.

**Copyright**© 2016 Solomon Tadesse, Yelda Bingöl Alpaslan, Mustafa Yıldız, Hüseyin Ünver and Kadir Aslan. This is an open-access article distributed under the terms of the Creative Commons Attribution License, which permits unrestricted use, distribution, and reproduction in any medium, provided the original author and source are credited.